

Raman investigation of $\text{YBa}_{2-x}\text{La}_x\text{Cu}_3\text{O}_7$ ceramics

R. Wegerer, C. Thomsen,* and M. Cardona

Max-Planck-Institut für Festkörperforschung, Heisenbergstrasse 1, D-70569 Stuttgart, Federal Republic of Germany

H. J. Bornemann† and D. E. Morris

Morris Research Inc., 1918 University Avenue, Berkeley, California 94704

(Received 13 April 1995; revised manuscript received 12 September 1995)

We present Raman data for the series of high-temperature superconducting compounds $\text{YBa}_{2-x}\text{La}_x\text{Cu}_3\text{O}_7$ with $x = 0, 0.1, 0.2, 0.3, 0.4,$ and 0.5 . We have investigated the dependence of frequencies and linewidths of the five Raman-active A_g modes on x . For $x=0.4$ a structural phase transition from orthorhombic to tetragonal takes place. With decreasing orthorhombicity $(a-b)/(a+b)$ the $\text{O}(2)\text{-O}(3)\text{-in-phase}$ and $\text{O}(2)\text{-O}(3)\text{-out-of-phase}$ modes increase their coupling, contrary to what one may expect. This can be understood in terms of a negative contribution of the chain fragments to the coupling matrix element between these two modes, which we estimate to be -52.9 cm^{-1} . With increasing x , two additional features become more pronounced in the Raman spectra. The first is a broad hump in the vicinity of the Ba peak and the second a peak at 570 cm^{-1} . Both peaks are assigned to a phonon-density-of-states contribution to the Raman spectra induced by the Ba-La disorder.

I. INTRODUCTION

Since the discovery of high- T_c superconductivity by Bednorz and Müller in 1986, a massive investigation of these materials by experimental and theoretical methods has taken place. Raman scattering is a powerful tool to study their phonons, the electronic continuum of excitations, and more recently crystal-field (CF) excitations of the rare-earth ions.¹⁻³ Here we report Raman studies of $\text{YBa}_{2-x}\text{La}_x\text{Cu}_3\text{O}_7$ materials with doping levels $x=0.0, 0.1, 0.2, 0.3, 0.4,$ and 0.5 . In particular, the frequency dependence on x of the coupled $\text{O}(2)\text{-O}(3)\text{-out-of-phase}$ and $\text{O}(2)\text{-O}(3)\text{-in-phase}$ modes are presented and interpreted on the basis of a simple model. This paper is structured as follows. In Sec. II we show the Raman spectra of $\text{YBa}_{2-x}\text{La}_x\text{Cu}_3\text{O}_7$ for the different doping levels. From these spectra, we evaluate how the frequencies and linewidths of the $5A_g$ modes and the observed B_{3g} mode evolve with increasing La concentration. In Sec. III a theoretical model for the frequency dependence of the $\text{O}(2)\text{-O}(3)\text{-out-of-phase}$ and the $\text{O}(2)\text{-O}(3)\text{-in-phase}$ modes on x is presented. Conclusions are drawn in Sec. IV.

II. EXPERIMENTAL RESULTS

Samples of $\text{YBa}_{2-x}\text{La}_x\text{Cu}_3\text{O}_7$ with $x = 0, 0.1, \dots, 0.5$ were prepared by solid-state reaction of Y_2O_3 , BaCO_3 , La_2O_3 , and CuO powders in flowing oxygen at a temperature of 950°C . By means of susceptibility measurements their T_c was determined to be 90, 85, 75, 55, 45, and 30 K for $x = 0.0, 0.1, 0.2, 0.3, 0.4,$ and 0.5 , respectively. This suppression of T_c is most likely due to the fact that the La ion has a nominal valence of $3+$, compared to $2+$ for the Ba which it replaces, and therefore reduces the hole concentration of the CuO_2 planes. The ionic radius of La^{3+} is 1.18 \AA and lies between those of Ba^{2+} (1.42 \AA) and Y^{3+} (1.02 \AA).⁴ Hence an isovalent substitution of Y^{3+} by La^{3+} is possible,

in principle, and found to take place for $x > 0.72$.⁵ Below we shall contend, on the basis of our Raman data, that indeed the La^{3+} ions occupy predominantly the Ba sites also for the doping concentrations $x < 0.5$ used here. Together with La doping it is possible to achieve oxygen contents higher than 7 in the samples as a result of the increase in free electron concentration provided by the $\text{Ba}^{2+} \rightarrow \text{La}^{3+}$ substitution. Karen *et al.*⁵ found the value $6.95+x$ for the upper limit of the oxygen content. A structural phase transition from the orthorhombic (D_{2h}) to the tetragonal (D_{4h}) point group occurs at $x=0.4$.

Bornemann and Morris⁶ have investigated the oxygen isotope effect in this class of materials and found a remarkably large isotope shift for low T_c values ($T_c \sim M^{-\alpha_0}$ with $\alpha_0 = 0.38$ for $T_c = 38.3\text{ K}$), which decreases gradually with increasing T_c up to 73 K and then falls rapidly to $\alpha_0 = 0.025$ for $T_c = 92.3\text{ K}$, the generally accepted value for $x=0$.⁷ They found the following expression for the dependence of the isotope-shift exponent on x :

$$\alpha_0 = 0.5[1 - T_c(x)/T_{c0}]^{0.59}, \quad (1)$$

with $T_{c0} = 92.8\text{ K}$. From these results a significant contribution of the phonons to the pairing mechanism was inferred.

In Fig. 1 we show Raman spectra of $\text{YBa}_{2-x}\text{La}_x\text{Cu}_3\text{O}_7$ ceramics for $x=0.0, 0.1, 0.2, 0.3, 0.4, 0.5$ at 300 K. One can clearly see for $x \geq 0.2$ a broad additional hump around the Ba and Cu modes increasing with x , which for $x=0.5$ extends to 250 cm^{-1} . Also an additional broad peak centered near 570 cm^{-1} is visible especially in the spectrum for $x > 0.3$. To identify these additional structures, we measured the oxygen-substituted ^{18}O sample ($\text{YLa}_{0.5}\text{Ba}_{1.5}\text{Cu}_3^{18}\text{O}_7$) (Fig. 2): It shows this peak at 537 cm^{-1} . The -6% frequency shift of this peak, with respect to that of the ^{16}O sample, indicates that oxygen motion is mainly responsible for this mode. Figure 3 displays the frequencies and linewidths [full width at

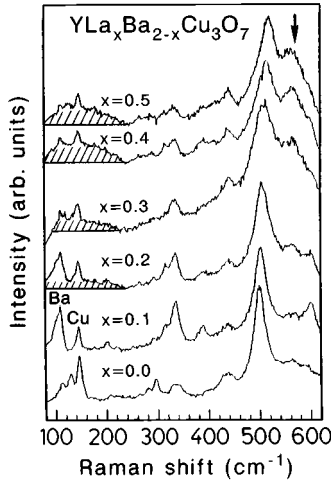


FIG. 1. Raman spectra of $\text{YLa}_x\text{Ba}_{2-x}\text{Cu}_3\text{O}_7$ ceramics for $x = 0.0, 0.1, \dots, 0.5$ at $T=300$ K. The shaded area and the vertical arrow indicate disorder-induced modes.

half maximum (FWHM)] obtained from fits to Lorentzian line shapes of the five A_g modes and one B_{3g} mode for the different doping levels.

III. DISCUSSION

From the data of Fig. 3 one can infer that La substitutes on the Ba and not on the Y sites. The argument is as follows: From the dependence of the frequency of the O(4) mode (apex oxygen at 500 cm^{-1} for $x=0$ and $R=Y$) and that the O(2)-O(3)-out-of-phase mode (335 cm^{-1}) in $\text{R}\text{Ba}_2\text{Cu}_3\text{O}_7$ ($R=\text{rare-earth ion}$) on the ionic radii of the rare-earth ion, which was investigated in Ref. 8, one can see that for the ionic radius of La^{3+} (1.18 \AA) the predicted frequency of the O(4) mode is at around 517 cm^{-1} , and that of the O(2)-O(3)-out-of-phase mode should lie near 283 cm^{-1} in $\text{La}\text{Ba}_2\text{Cu}_3\text{O}_7$. In our samples the O(4) mode shifts with increasing La concentration to higher frequency while the O(2)-O(3)-out-of-phase mode stays almost constant. If La were to go to the rare-earth position, the O(2)-O(3)-out-of-phase mode would also shift towards lower frequencies; however, within the experimental scatter of $\pm 1 \text{ cm}^{-1}$ its

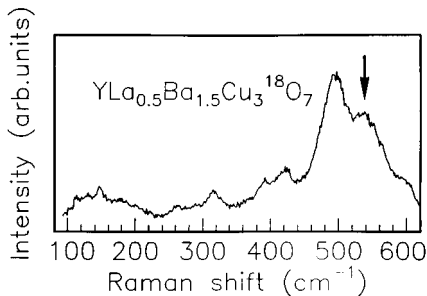


FIG. 2. Raman spectrum of a $\text{YLa}_{0.5}\text{Ba}_{1.5}\text{Cu}_3^{18}\text{O}_7$ ceramic sample. The vertical arrow indicates a disorder-induced mode.

frequency remains constant. There is another hint suggesting that La sits on the Ba places: Friedl *et al.* investigated the frequency dependence of the B_{3g} mode [O(4) motion in the y direction] on the ionic radius.⁹ They found that this mode shifts considerably towards lower frequencies with increasing rare-earth radius, from 310 cm^{-1} for $r = 1.00 \text{ \AA}$ (Tm^{3+}) to $\approx 284 \text{ cm}^{-1}$ for $r = 1.14 \text{ \AA}$ (Pr^{3+}). Upon the $\text{Ba} \rightarrow \text{La}$ substitution performed here, however, this mode stays constant for the different substitution levels, especially up to $x=0.4$.

As already mentioned, the phase transition from orthorhombic to tetragonal symmetry takes place⁴ at $x=0.4$. For $x < 0.4$ the a - and b -axis lengths change by similar amounts in opposite directions. Hence we can estimate the Grüneisen parameter γ_i of the various modes from the data in Fig. 3 by assuming that the contributions of a - and b -axis lengths nearly cancel. Hence, γ_i for a vibration along c can be approximated by

$$\gamma_i = -\frac{\partial \ln \omega_i(V)}{\partial \ln(V)} \cong -\frac{1}{3} \frac{\partial \ln \omega_i(c)}{\partial \ln(c)} = -\frac{1}{3} \frac{\partial \omega_i(c)/\omega_i}{\partial c/c}, \quad (2)$$

where i denotes the specific phonon under consideration.

From our spectra (Fig. 3) we evaluate the relative frequency shifts $(\Delta\omega/\omega)(\text{Ba}) \cong 2.7\%$, $(\Delta\omega/\omega)[\text{Cu}(2)] \cong 1.4\%$, $(\Delta\omega/\omega)[\text{O}(2,3)\text{-out-of-phase mode}] \cong 0\%$, $(\Delta\omega/\omega)[\text{O}(2,3)\text{-in-phase mode}] \cong 1.1\%$, and $(\Delta\omega/\omega)[\text{O}(4)] \cong 3.6\%$ towards higher values with a c -axis contraction of about 1% with La concentration⁴ increasing from $x=0$ to $x=0.5$. Evaluating γ_i one sees that the Ba mode and the O(4) mode show the typical frequency shifts, whereas the Cu(2) mode reveals a somewhat too small mode-Grüneisen parameter.

Now we discuss the frequency behavior of the O(2,3)-in-phase- and O(2,3)-out-of-phase A_g modes: As mentioned above, the O(2)-O(3)-out-of-phase mode does not vary with La concentration. These modes, which have different symmetries and thus do not mix for perfectly tetragonal crystals (D_{4h} point group), should mix when the symmetry is lowered to D_{2h} . Local density approximation (LDA) calculations show that the O(2)-O(3)-in-phase and the O(2)-O(3)-out-of-phase mode mixing is considerable in the D_{2h} -point group.¹⁰ When these modes become decoupled as a result of the phase transition from D_{2h} to D_{4h} one should, with increasing decoupling, observe a frequency shift of the O(2)-O(3)-out-of-phase mode towards higher frequencies. The reduction of the c axis should enhance this trend. Let us illustrate this fact quantitatively.

We denote the two phonon states in the tetragonal, decoupled case by $|1\rangle = (1/\sqrt{2})(|a\rangle + |b\rangle)$ and $|2\rangle = (1/\sqrt{2}) \times (|a\rangle - |b\rangle)$, where $|1\rangle$ represents the in-phase A_{1g} mode and $|2\rangle$ the out-of-phase B_{1g} mode (tetragonal notation). The state $|a\rangle$ represents the vibration of the O(2) atom (a axis) and $|b\rangle$ stands for the vibration of the O(3) atom (b axis) along the z direction. States $|a\rangle$ and $|b\rangle$ result from a 50% mixing of the basis states $|1\rangle$ and $|2\rangle$. The Hamiltonian of the coupled modes can be written in the representation defined by $|1\rangle$ and $|2\rangle$ as

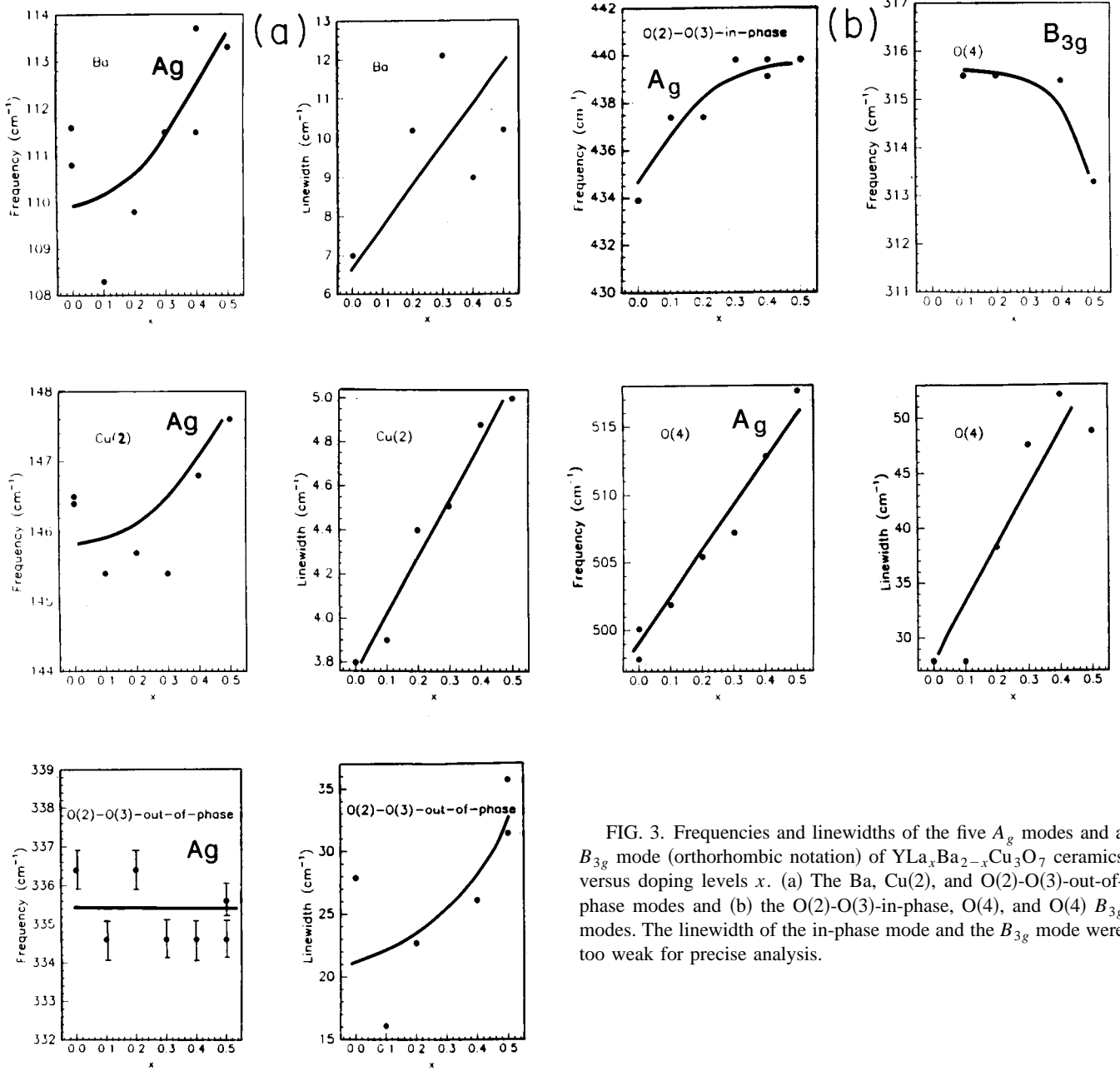


FIG. 3. Frequencies and linewidths of the five A_g modes and a B_{3g} mode (orthorhombic notation) of $\text{YLa}_x\text{Ba}_{2-x}\text{Cu}_3\text{O}_7$ ceramics versus doping levels x . (a) The Ba, Cu(2), and O(2)-O(3)-out-of-phase modes and (b) the O(2)-O(3)-in-phase, O(4), and O(4) B_{3g} modes. The linewidth of the in-phase mode and the B_{3g} mode were too weak for precise analysis.

$$H = \begin{pmatrix} \frac{\omega_1^0 + \omega_2^0}{2} + k_T & k_\alpha + k_\beta \\ k_\alpha + k_\beta & \frac{\omega_1^0 + \omega_2^0}{2} - k_T \end{pmatrix}. \quad (3)$$

In Eq. (3), ω_1^0 and ω_2^0 are the frequencies of the decoupled (tetragonal) modes, $2k_T$ represents their separation in energy in the tetragonal phase, k_α denotes the coupling due to the presence of the CuO chains or chain fragments which exist even for $a=b$, and k_β denotes the coupling because of the $a \neq b$ orthorhombic distortion of the unit cell.

In order to account for the experimental dependence of the A_{1g} ($\sim 434 \text{ cm}^{-1}$) and B_{1g} ($\sim 335 \text{ cm}^{-1}$) modes (tetragonal notation) shown in Fig. 3 we make the assumption that in the tetragonal phase ($x = 0.5$) at least fragments of CuO chains still exist which locally break the tetragonal

symmetry. In this manner Eq. (3) remains valid with $k_\beta = 0$ (since $a=b$) but $k_\alpha \neq 0$. The increase in the A_{1g} - B_{1g} frequency separation observed at $x=0.5$ will automatically obtain, provided k_α and k_β have opposite signs in the ‘‘orthorhombic’’ phase ($x \approx 0$). We estimate next k_α and k_β including their sign. We write the eigenvectors of (3) as

$$|1'\rangle = \alpha|1\rangle - \beta|2\rangle, \quad |2'\rangle = \beta|1\rangle + \alpha|2\rangle. \quad (4)$$

Using Eq. (3) we obtain for the frequency splitting Ω the $|1'\rangle, |2'\rangle$ modes

$$\Omega = 2\sqrt{k_T^2 + (k_\alpha + k_\beta)^2}. \quad (5)$$

Using Eq. (4) the coupling constant k_T can be obtained from the eigenvector components α and β with the equation

$$k_T = \frac{\Omega}{2} \left(\frac{(\alpha/\beta)^2 - 1}{(\alpha/\beta)^2 + 1} \right). \quad (6)$$

We use $\Omega = 99 \text{ cm}^{-1}$ for the determination of k_T as obtained from Fig. 3 for $x=0$. For the ratio α/β we take the value calculated from the *ab initio* linear muffin-tin orbital (LMTO) band structure in Ref. 10 using the frozen phonon method ($\alpha/\beta=1.73$) (note that the eigenvectors of Ref. 10 include some admixture of apical oxygen motion which we neglect here). We thus find $k_T = 24.7 \text{ cm}^{-1}$. Replacing this value into (5) we obtain $k_\alpha + k_\beta = -42.9 \text{ cm}^{-1}$, the sign being determined by the condition $\alpha^2 + \beta^2 = 1$.

We make next an attempt to separate the individual contributions of k_α and k_β to $k_\alpha + k_\beta$. For this purpose it is useful to make a basis transformation from the states $|1\rangle$ and $|2\rangle$ to the states $|a\rangle$ and $|b\rangle$ and write the Hamiltonian of Eq. (3) in this new representation as

$$H = \begin{pmatrix} \frac{\omega_1^0 + \omega_2^0}{2} + k_\alpha + k_\beta & k_T \\ k_T & \frac{\omega_1^0 + \omega_2^0}{2} - k_\alpha - k_\beta \end{pmatrix}. \quad (7)$$

We make the reasonable assumption that k_β is determined by the difference in lengths of the a and b axes. This follows, to first order, from the assumption that the frequency of the vibration $|a\rangle$ depends only on the length of a and that of $|b\rangle$ on b .

The change in energy of the state $|a\rangle$ for a distortion $da = -db$ is given by

$$\delta \langle a | H_0 | a \rangle = \langle a | \delta H_0 | a \rangle \approx - \frac{\omega_1^0 + \omega_2^0}{2} \frac{3}{2} \left(\frac{da}{a} - \frac{db}{b} \right), \quad (8)$$

where we assumed that the relative change in mode frequency is 3 times that of the relative length of the corresponding bond, i.e., a ‘‘Grüneisen parameter’’ of 1.

With a distortion of -1.2% of the lattice constant a and of $+0.65\%$ of b during the transition from tetragonal to orthorhombic symmetry⁴ $k_\beta = +10 \text{ cm}^{-1}$ results from Eq. (8). Using this value of k_β and $k_\alpha + k_\beta = -42.9 \text{ cm}^{-1}$, as given above, we find $k_\alpha = -52.9 \text{ cm}^{-1}$, thus confirming our conjecture that k_α and k_β have opposite signs. From these values of k_T , k_α , and k_β we find

$$\omega'_1 = 386 + \sqrt{k_T^2 + (k_\alpha + k_\beta)^2} = 435.5 \text{ cm}^{-1} \text{ for } x=0,$$

$$\omega'_1 = 386 + \sqrt{k_T^2 + k_\alpha^2} = 444.4 \text{ cm}^{-1} \text{ for } x=0.5.$$

These frequencies are in good agreement with the results of Fig. 3. We should point out that the calculated effect may be reduced if the oxygen concentration increases with increas-

ing x . It is, however, possible to model oxygen configurations in which this effect is kept to a minimum; in particular, it is by no means clear that the additional oxygen forms chains. Because of our lack of knowledge about the concentration and structure of the excess oxygen, we do not treat this effect explicitly.

Finally, we discuss the appearance of the broad hump in the low-frequency parts of the spectra. The hump near the Ba mode frequency (shaded area in Fig. 1) is presumably due to disorder, i.e., multiple folding of the Brillouin zone, which causes additional modes at the Γ point. This becomes more evident by considering the phonon density of states of $\text{YBa}_2\text{Cu}_3\text{O}_7$ measured by neutron scattering¹¹ which also has a minimum at 280 cm^{-1} . Furthermore, one also expects a broadening of the different modes because of disorder, which is especially visible for the O(2)-O(3)-out-of-phase mode and the O(4) mode (Fig. 3).

IV. CONCLUSION

We have reported Raman measurements on $\text{YBa}_{2-x}\text{La}_x\text{Cu}_3\text{O}_7$ ceramic samples for $x = 0.0, 0.1, 0.2, 0.3, 0.4,$ and 0.5 . The frequencies and linewidths of the observed phonons have been investigated. The linewidths show a broadening due to disorder and the frequencies reveal shifts which correspond to mode-Grüneisen parameters of 1–1.5, as usually expected. A broad hump near the Ba mode and another broad peak at 570 cm^{-1} , which are most pronounced in the sample with $x=0.5$, are assigned to additional phonon-density-of-states scattering by comparing it with the measured phonon density of states of $\text{YBa}_2\text{Cu}_3\text{O}_7$ and with the spectrum of an ^{18}O -substituted sample. In the latter sample the peak at 570 cm^{-1} exhibits an isotopic shift of -6% , indicating an oxygen vibration. By increasing the La concentration, a phase transition from orthorhombic to tetragonal symmetry occurs at $x=0.4$. At the same time, and surprisingly at first sight, the energy separation of the O(2)-O(3)-in-phase mode and the O(2)-O(3)-out-of-phase mode increases, which, contrary to the simplest symmetry considerations, implies an increased coupling for tetragonal symmetry.

From the frequency shifts of those modes and also from Grüneisen parameter considerations, a coupling constant $k_\beta = +10 \text{ cm}^{-1}$ has been evaluated for the effect of the orthorhombic distortion of the unit cell and a negative one of $k_\alpha = -52.9 \text{ cm}^{-1}$ for the effect of the chain fragments.

ACKNOWLEDGMENTS

Thanks are due to H. Hirt, M. Siemers, and P. Wurster for expert technical help. We gratefully acknowledge financial support from the Bundesminister für Forschung und Technologie under Grant No. 13N5840 5 and the European Union, Science program under Grant No. SC1*CT910751.

*Present address: Inst. für Festkörperphysik, PN 5-4, TU Berlin, Hardenbergstr. 36, 10623 Berlin, Germany.

†Present address: KFK-Karlsruhe GmbH, Postfach 3640, 76021 Karlsruhe, Germany.

¹E.T. Heyen, R. Wegerer, E. Schönherr, and M. Cardona, Phys. Rev. B **44**, 10 195 (1991).

²R. Wegerer, C. Thomsen, T. Ruf, E. Schönherr, and M. Cardona, Phys. Rev. B **48**, 6413 (1993).

- ³S. Jandl, M. Iliev, C. Thomsen, T. Ruf, M. Cardona, B.M. Wanklyn, and C.-K. Cheng, *Solid State Commun.* **87**, 609 (1993).
- ⁴R.J. Cava, B. Batlogg, R.M. Fleming, S.A. Sunshine, A. Ramirez, E.A. Rietmann, S.M. Zakurah, and R.B. van Dover, *Phys. Rev. B* **37**, 5912 (1988).
- ⁵P. Karen, H. Fjelliåg, A. Kjekshus, and A.F. Andersen, *J. Solid State Chem.* **93**, 163 (1991).
- ⁶H.J. Bornemann and D.E. Morris, *Phys. Rev. B* **44**, 5322 (1991).
- ⁷D.M. Ginsberg, in *Physical Properties of High Temperature Superconductors IV*, edited by J.P. Franck (World Scientific, Singapore, 1994), p. 189.
- ⁸M. Cardona, R. Liu, C. Thomsen, M. Bauer, L. Genzel, W. König, A. Wittlin, U. Amador, M. Barahona, F. Fernandez, C. Otero, and R. Saez, *Solid State Commun.* **65**, 71 (1988).
- ⁹B. Friedl, C. Thomsen, E. Schönherr, and M. Cardona, *Solid State Commun.* **76**, 1107 (1990).
- ¹⁰C.O. Rodríguez, A.I. Liechtenstein, I.I. Mazin, O. Jepsen, O.K. Andersen, and M. Methfessel, *Phys. Rev. B* **42**, 2691 (1990).
- ¹¹B. Renker, F. Gompf, E. Gering, D. Evert, H. Rietschel, and A. Dianoux, *Z. Phys. B* **71**, 309 (1988).